Chambers et al.,http://www.jcb.org/cgi/content/full/jcb.201202005/DC1

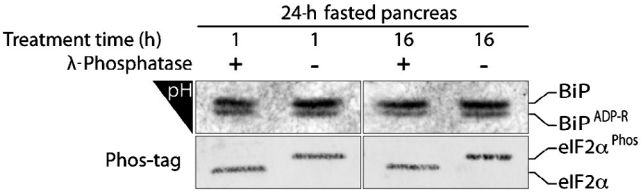

Figure S1. **The acidic form of BiP is not affected by phosphatase in vitro.** IEF blot of BiP from a fasted mouse incubated for the indicated period of time with λ-phosphatase or buffer alone (top). A control reaction containing in vitro phosphorylated eIF2α (eIF2α^{Phos}) was resolved on a Phos-tag gel (bottom). The experiment shown was performed once.

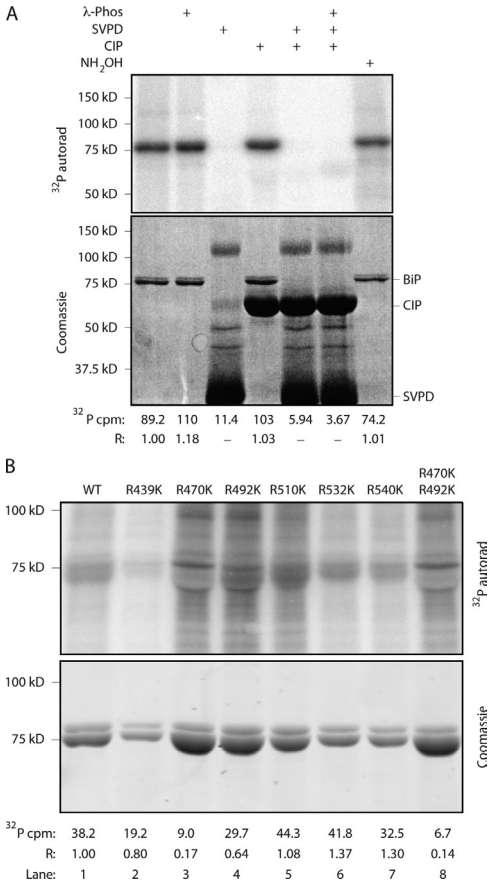

Figure S2. **^{32}P-metabolic labeling of BiP survives phosphatase and hydroxylamine treatment in vitro and is limited to two Arg residues.** (A) Autoradiograph (autorad) and Coomassie stain of ^{32}P-labeled FLAG-tagged BiP immunopurified from ^{32}P-orthophosphate–labeled 293T cells. Where indicated, samples were exposed in vitro to λ-phosphatase (λ-Phos), snake venom phosphodiesterase (SVPD) CIP, or NH_2OH before separation by SDS-PAGE and autoradiography. (B, top) Autoradiograph of ^{32}P-labeled wild type (WT) and the indicated FLAG-tagged mutant BiP immunopurified from ^{32}P-orthophosphate–labeled 293T cells. (bottom) Coomassie stain of the same gel. ^{32}P-radioactive counts (after background subtraction) and counts normalized to BiP protein content in each sample (R) are indicated. A representative experiment reproduced twice is shown.

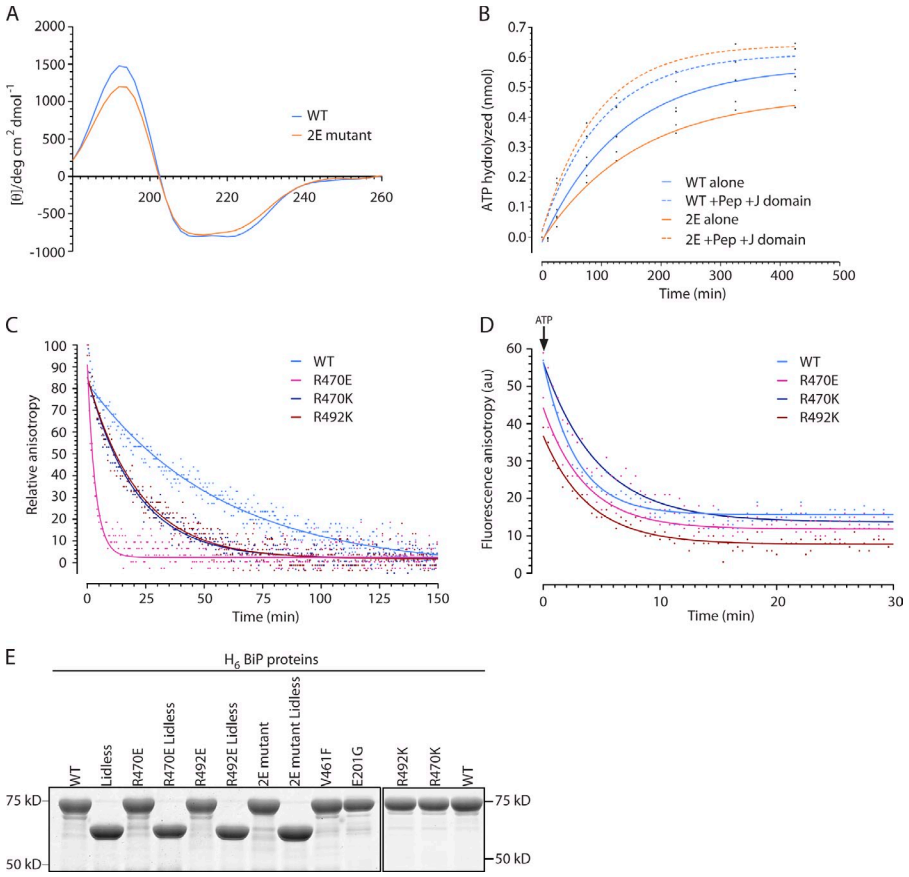

Figure S3. **Structural and functional integrity of the mutant BiP proteins in vitro.** (A) Comparison of the CD spectra of purified, bacterially expressed wild-type (WT) and BiP$^{R470E;R492E}$ double mutant (2E) BiP. (B) Time-dependent trace of ATP hydrolysis during the course of the experiment by 25 pmol of wild-type or BiP$^{R470E;R492E}$ double mutant BiP in the absence and presence of 30 µM substrate peptide (Pep) and 2 µM P58 J-domain (the ADP signal at $t = 0$ was subtracted from all experimental points). A representative experiment reproduced twice is shown. (C) Time-dependent changes in relative fluorescent anisotropy of Lucifer yellow–labeled BiP substrate peptide (NH2-HTFPAVLGSC-COOH) bound at steady state to the indicated BiP proteins (in the presence of 1 mM ADP) after introduction of a 500-fold excess of unlabeled peptide at $t = 0$. A representative experiment reproduced three times is shown. (D) Fluorescent anisotropy signal of the BiP-bound–labeled peptide (in the presence of 1 mM ADP, as in C) after introduction of an excess of ATP (4 mM) at $t = 0$. au, arbitrary unit. (E) Coomassie-stained SDS-PAGE of the proteins used or biochemical assays.

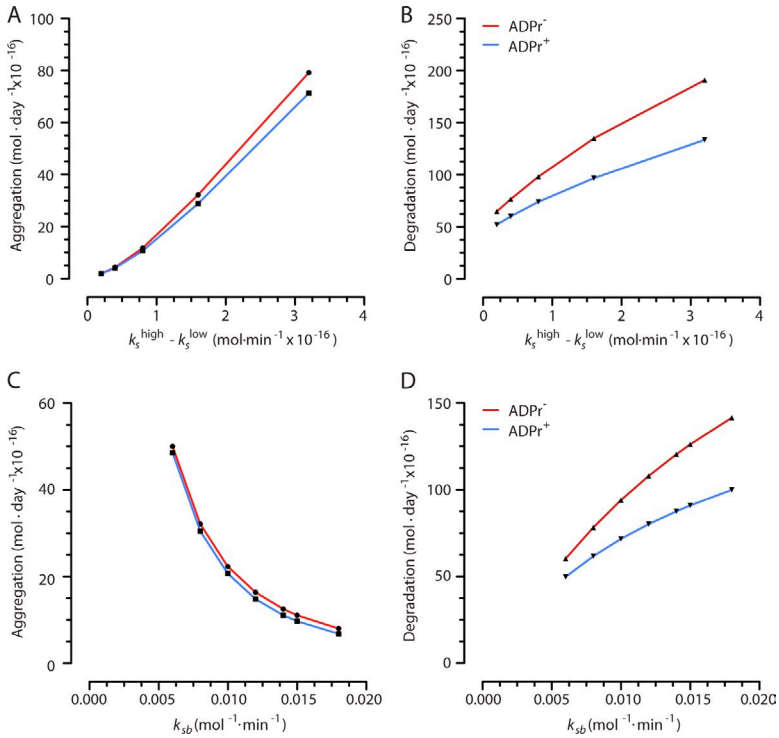

Figure S4. **The advantages of the ADPr$^+$ model over the ADPr$^-$ model are maintained over a range of diurnal excursions in protein synthesis rates and a range of gains of the transcriptional UPR.** (A) Comparison of aggregation of U over a 24-h cycle in the ADPr$^-$ and ADPr$^+$ model at various diurnal excursions of low- and high-synthesis rates of unfolded proteins. (B) Comparison of degradation over a 24-h cycle in the ADPr$^-$ and ADPr$^+$ model at various diurnal excursions of low- and high-synthesis rates of unfolded proteins. (C) Comparison of aggregation of U over a 24-h cycle in the ADPr$^-$ and ADPr$^+$ models at various values of k_{sb}. (D) Comparison of degradation of U over a 24-h cycle in the ADPr$^-$ and ADPr$^+$ models at various values of k_{sb}.

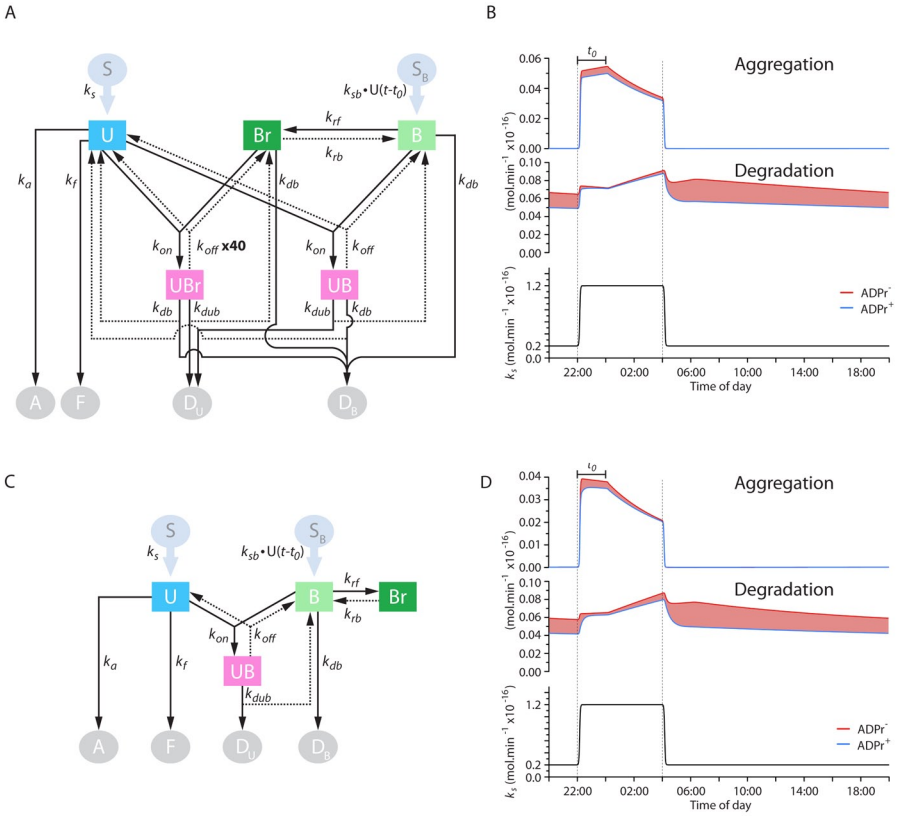

Figure S5. **Alternative ADPr⁺ models for substrate-binding activity of ADP-ribosylated BiP and BiP degradation also afford an advantage over an ADPr⁻ model.** (A) Schema of the kinetic model of the ER. Unfolded proteins (U) are introduced into the ER at variable rates (k_s) from a source (S). In the ER, they can fold (to F, with a rate constant k_f), misfold, and aggregate (to A, with a rate constant k_a) or bind with BiP (B), forming a reversible complex (UB, with a forward rate constant k_{on} and a reverse rate constant k_{off}) or a functionally identical complex with ADP-ribosylated BiP (UBr, with the same forward rate constant k_{on} and a reverse rate constant that is 40 times greater than k_{off} of the UB complex). The unfolded protein in the UB and UBr complexes can be degraded (to D_u, with rate constant k_{dub}), releasing unmodified BiP (B) or ADP-ribosylated BiP (Br). The production of BiP is proportional to the burden of unfolded protein in the ER and set by the rate constant k_{sb}. The delay factor t_0 models the latency of the transcriptionally based UPR. BiP is turned over by degradation of B (to D_B, with rate constant k_{db}). Degradation of BiP from complex with substrate (UB and UBr) liberates free U. In the ADPr⁺ model, B is in a dynamic equilibrium with its ADP-ribosylated form Br (governed by the rate constants k_{rf} and k_{rb}). (B) Comparison of the time evolution of the rates of aggregation and degradation of unfolded protein in the ADPr⁻ and ADPr⁺ models described in A. The red shading highlights surplus aggregation or degradation of unfolded proteins in the ADPr⁻ model. Note the dominance of the red trace in aggregation during the high-synthesis phase of the diurnal variation in translation (top) and in degradation during the low-synthesis phase of the cycle. The latent phase of the response of BiP synthesis to changes in the burden of unfolded proteins is indicated by the bar (t_0). (C) A modified kinetic model in which only free BiP contributes to its degradation. (D) Comparison of the time evolution of the rates of aggregation and degradation of unfolded protein in the ADPr⁻ and ADPr⁺ models (as in B).